CERN-PH-TH/2009-171

The V-mode polarization of the Cosmic Microwave Background

Massimo Giovannini [1]

Department of Physics, Theory Division, CERN, 1211 Geneva 23, Switzerland

INFN, Section of Milan-Bicocca, 20126 Milan, Italy

Abstract

The V-mode polarization of the Cosmic Microwave Background is discussed in a weakly magnetized plasma. The VV and VT angular power spectra are computed for adiabatic initial conditions of the Einstein-Boltzmann hierarchy. Depending upon the frequency channel and upon the magnetic field intensity, the VT power spectra of the circular polarization can even be seven orders of magnitude larger than a putative B-mode polarization stemming from the lensing of the primary anisotropies. Specific programs aimed at the direct detection of the V-mode polarization of the Cosmic Microwave Background could provide a new observational tool for the scrutiny of pre-decoupling physics.

[1] Electronic address: massimo.giovannini@cern.ch

The spectral energy density (per logarithmic interval of frequency) of the Cosmic Microwave Background (CMB in what follows) is maximal, today, for photon energies $E_\gamma \sim 9.2 \times 10^{-4}$ eV whose associated wavelength $\lambda_\gamma \sim 2\pi/E_\gamma$ is of the order of 0.13 mm. According to the WMAP 5-yr data the redshift of hydrogen recombination can be estimated approximately as $z_{\rm rec} = 1090.51 \pm 0.95$ [1] corresponding to the conformal time[2] $\tau_{\rm rec}$; at $\tau_{\rm rec}$ the maximum of the CMB is $z_{\rm rec} E_\gamma \simeq$ eV corresponding to a physical wavelength $\lambda_\gamma(\tau_{\rm rec}) = \lambda_\gamma/z_{\rm rec} \simeq 0.12\,\mu$m. Prior to recombination the electrons and the ions have kinetic temperatures which are comparable with the temperature of the photons, i.e. $(1 + z_{\rm rec})T_{\gamma 0}$ (where $T_{\gamma 0} = 2.725\,{\rm K}$). The small difference between electron and proton temperatures is controlled by the ratio between the Hubble rate H and the Coulomb rate $\Gamma_{\rm Coul}$ which is $\mathcal{O}(10^{-11})$ at $\tau_{\rm rec}$. The global charge neutrality of the plasma combined with the baryon asymmetry implies that the electron and proton concentrations are equal and both of the order of $10^{-10}\, n_\gamma$ where n_γ is the comoving photon concentration. Prior to recombination the plasma is cold: the electron and proton masses are both much larger than the kinetic temperature of the corresponding species. Consider the physical situation when, prior to recombination, the plasma is supplemented by a magnetic field whose typical inhomogeneity scale is at least comparable (and possibly even larger) than the Hubble radius H^{-1} at the corresponding epoch. Since the wavelengths of the scattered photons are minute in comparison with the Hubble radius (i.e. $\lambda_\gamma(\tau_{\rm rec}) \ll H^{-1}$) the magnetic field gradients can be ignored, in the first approximation, when computing the photon-electron (and photon-ion) scattering. The gradient expansion on the magnetic field strength was termed long ago by Alfvén guiding centre approximation [2].

Having introduced $\hat{e}_1$ and $\hat{e}_2$ as two mutually orthogonal directions (both perpendicular to the direction of propagation of the radiation), and recalling the standard definitions of the Stokes parameters [3] it can be easily shown that

$$I = |\vec{E}\cdot\hat{e}_1|^2 + |\vec{E}\cdot\hat{e}_2|^2, \qquad V = 2\,{\rm Im}[(\vec{E}\cdot\hat{e}_1)^*(\vec{E}\cdot\hat{e}_2)], \tag{1}$$

are both invariant for a rotation of $\hat{e}_1$ and $\hat{e}_2$ on the plane orthogonal to the direction of propagation of the radiation. For the same two-dimensional rotation, $(Q \pm iU)$ transform as a function of spin weight ∓ 2 on the two-sphere [4]; this observation leads, after some algebra, to the known form of the E-mode and B-mode polarization [5]. If a large-scale magnetic field is present and if, concurrently, the spatial curvature does fluctuate over large scales, then the power spectra associated with the brightness perturbations of V will not be vanishing and shall be defined, in what follows, V-mode power spectra in analogy with the B-mode and E-mode power spectra characterizing the linear polarizations.

[2]The conformal time coordinate τ will be used throughout; in terms of τ the background metric $\overline{g}_{\mu\nu}$ will be chosen as conformally flat i.e. $\overline{g}_{\mu\nu} = a^2(\tau)\eta_{\mu\nu}$ where $\eta_{\mu\nu} = {\rm diag}(1, -1, -1, -1)$ is the Minkowski metric. The current observational evidence [1] suggests, indeed, that the spatial curvature can be neglected at the recombination epoch, at least in the framework of the concordance model, i.e. the ΛCDM paradigm where Λ stands for the dark energy component and CDM stands for the cold dark matter contribution.

To compute the induced V-mode polarization the evolution of the brightness perturbations must be written in the case when the photons scatter electrons in a magnetized background. In the elastic e-γ scattering occurring in a cold plasma the recoil energy of the electron can be neglected [6]; photons impinging on electrons and ions in a weakly magnetized medium can be described, as usual, in terms of a scattering matrix connecting the outgoing to the ingoing Stokes parameters (see, e.g. [3]). The latter step will lead, after angular integration, to the evolution of the various brightness perturbations[3]

$$\Delta_{\rm I}' + ik\mu(\Delta_{\rm I} + \phi) + \epsilon'\Delta_{\rm I} = \psi' + \epsilon'\mathcal{C}_{\rm I}(\omega, k, \mu), \tag{2}$$

$$\Delta_{\rm P}' + ik\mu\Delta_{\rm P} + \epsilon'\Delta_{\rm P} = \epsilon'\mathcal{C}_{\rm P}(\omega, k, \mu), \tag{3}$$

$$\Delta_{\rm V}' + ik\mu\Delta_{\rm V} + \epsilon'\Delta_{\rm V} = \epsilon'\mathcal{C}_{\rm V}(\omega, k, \mu), \tag{4}$$

where the prime denotes a derivation with respect to the conformal time coordinate τ while $\phi = \delta_{\rm s}^{(1)} g_{00}/(2a^2)$ and $\psi\delta_{ij} = \delta_{\rm s}^{(1)} g_{ij}/(2a^2)$ are the scalar fluctuations of the metric whose relation to the curvature fluctuations can be expressed, in the longitudinal gauge, as

$$\mathcal{R} = -\psi - \frac{\mathcal{H}^2}{\mathcal{H}^2 - \mathcal{H}'}\biggl(\phi + \frac{\psi'}{\mathcal{H}}\biggr), \qquad \mathcal{H} = \frac{a'}{a}; \tag{5}$$

note that the relation of $\mathcal{H}$ to the Hubble parameter is simply given by $aH = \mathcal{H}$; the source functions appearing in Eqs. (2), (3) and (4) are given by

$$\begin{aligned}
\mathcal{C}_{\rm I}(\omega, k, \mu) = {} & \frac{1}{4}\biggl\{\Delta_{\rm I0}\biggl[2\Lambda_3(\omega)(1-\mu^2) + 2\zeta^2(\omega)\biggl(\mu^2 + \Lambda_1^2(\omega) + f_{\rm e}^2(\omega)\Lambda_1^2(\omega)(1+\mu^2)\biggr)\biggr] \\
& + \biggl[2\Lambda_3(\omega)(1-\mu^2) - \zeta^2(\omega)\biggl(\mu^2 + \Lambda_1^2(\omega)\biggr) - f_{\rm e}^2(\omega)\zeta^2(\omega)\Lambda_2^2(\omega)(1+\mu^2)\biggr] S_{\rm P} + 4\mu v_{\rm b} \\
& - 6\, i\, f_{\rm e}^2(\omega)\zeta^2(\omega)\Lambda_2(\omega)\biggl[\mu^2 + \Lambda_1(\omega)\biggr]\Delta_{\rm V1}\biggr\},
\end{aligned} \tag{6}$$

$$\begin{aligned}
\mathcal{C}_{\rm P}(\omega, k, \mu) = {} & \frac{1}{4}\biggl\{\biggl[2(1-\mu^2)\biggl(\Lambda_3(\omega) - \zeta^2(\omega) f_{\rm e}^2(\omega)\Lambda_2^2(\omega)\biggr) - 2\zeta^2(\omega)\biggl(\Lambda_1(\omega) - \mu^2\biggr)\biggr]\Delta_{\rm I0} \\
& + \biggl[2\Lambda_3(\omega)(1-\mu^2) - \zeta^2(\omega)\biggl(\mu^2 - \Lambda_1^2(\omega) - f_{\rm e}^2(\omega)\Lambda_2^2(\omega)(1-\mu^2)\biggr)\biggr] S_{\rm P} \\
& - 6 i f_{\rm e}^2(\omega)\zeta^2(\omega)\Lambda_2(\omega)\biggl(\mu^2 - \Lambda_1(\omega)\biggr)\Delta_{\rm V1}\biggr\},
\end{aligned} \tag{7}$$

$$\begin{aligned}
\mathcal{C}_{\rm V}(\omega, k, \mu) = {} & \frac{\zeta^2(\omega) P_1(\mu)}{2}\biggl\{f_{\rm e}(\omega)\Lambda_2(\omega)\biggl(\Lambda_1(\omega) + 1\biggr)\biggl[2\Delta_{\rm I0} - S_{\rm P}\biggr] \\
& - \frac{3}{2} i\biggl[\Lambda_1(\omega) + f_{\rm e}^2(\omega)\Lambda_2^2(\omega)\biggr]\Delta_{\rm V1}\biggr\},
\end{aligned} \tag{8}$$

where the dependence upon the frequency of the observational channel arises through the functions

$$\Lambda_1(\omega) = 1 + \biggl(\frac{\omega_{\rm p\,i}^2}{\omega_{\rm p\,e}^2}\biggr)\biggl(\frac{\omega^2 - \omega_{\rm B\,e}^2}{\omega^2 - \omega_{\rm B\,i}^2}\biggr), \quad \Lambda_2(\omega) = 1 - \biggl(\frac{\omega_{\rm p\,i}^2}{\omega_{\rm p\,e}^2}\biggr)\biggl(\frac{\omega_{\rm B\,i}}{\omega_{\rm B\,e}}\biggr)\biggl(\frac{\omega^2 - \omega_{\rm B\,e}^2}{\omega^2 - \omega_{\rm B\,i}^2}\biggr),$$

[3]In what follows $\epsilon' = a x_{\rm e} \tilde{n}_0 \sigma_{\gamma{\rm e}}$ is the differential optical depth, $\tilde{n}_0 = n_0/a^3$ is the physical concentration and $\sigma_{\gamma{\rm e}} = (8/3)\pi(e^2/m_{\rm e})^2$. The quantity μ is simply the projection of the Fourier wavevector on the direction of the photon momentum.

$$\Lambda_3(\omega) = 1 + \biggl(\frac{\omega_{\rm p\,i}^2}{\omega_{\rm p\,e}^2}\biggr), \quad \zeta(\omega) = \frac{1}{f_{\rm e}^2(\omega) - 1} = \frac{\omega^2}{\omega_{\rm Be}^2 - \omega^2}, \quad f_{\rm e}(\omega) = \biggl(\frac{\omega_{\rm B\,e}}{\omega}\biggr). \tag{9}$$

The plasma and Larmor frequencies for electrons and ions are denoted, respectively, by $(\omega_{\rm p\,e},\, \omega_{\rm B\,e})$ and $(\omega_{\rm p\,i},\, \omega_{\rm B\,i})$. CMB experiments operate for angular frequencies which are typically larger than the Larmor[4] and plasma frequencies of the electrons at recombination; it is therefore legitimate to expand the source functions of Eqs. (2), (3) and (4) in powers of $f_{\rm e}(\omega) = (\omega_{\rm B\,e}/\omega)$ as well as in powers of $(m_{\rm e}/m_{\rm p})$; the result of this double expansion can be written as

$$\mathcal{C}_{\rm I}(\omega, k, \mu) = \biggl[\Delta_{\rm I0} + \mu v_{\rm b} - \frac{P_2}{2} S_{\rm P}\biggr]$$
$$+ [2 + P_2(\mu)] f_{\rm e}^2(\omega) \biggl[\Delta_{\rm I0} - i\Delta_{\rm V1} - \frac{S_{\rm P}}{2}\biggr] + \mathcal{O}\biggl(\frac{m_{\rm e}}{m_{\rm p}}\biggr) + \mathcal{O}(f_{\rm e}^4), \tag{10}$$

$$\mathcal{C}_{\rm P}(\omega, k, \mu) = \frac{1 - P_2(\mu)}{2} \biggl\{ S_{\rm P} + f_{\rm e}^2(\omega) \biggl[2i\Delta_{\rm V1} - 2\Delta_{\rm I0} + S_{\rm P}\biggr]\biggr\}$$
$$+ \mathcal{O}\biggl(\frac{m_{\rm e}}{m_{\rm p}}\biggr) + \mathcal{O}(f_{\rm e}^4), \tag{11}$$

$$\mathcal{C}_{\rm V}(\omega, k, \mu) = \frac{P_1(\mu)}{2} \biggl\{ 2 f_{\rm e}(\omega) \biggl[2\Delta_{\rm I0} - S_{\rm P}\biggr] - \frac{3}{2} i \biggl[1 + f_{\rm e}^2(\omega)\biggr] \Delta_{\rm V1}\biggr\}$$
$$+ \mathcal{O}\biggl(\frac{m_{\rm e}}{m_{\rm p}}\biggr) + \mathcal{O}(f_{\rm e}^4), \tag{12}$$

where $P_\ell(\mu)$ is the Legendre polynomial of ℓ-th order and where $S_{\rm P}(k, \tau) = (\Delta_{\rm P0} + \Delta_{\rm P2} + \Delta_{\rm I2})$ is the standard source term for the E-mode polarization when $f_{\rm e}(\omega) = 0$. Indeed, in the limit $f_{\rm e}(\omega) \to 0$, Eqs. (2), (3) and (4) reproduce the standard results for the evolution equations of the scalar brightness perturbations. The source functions obtained in Eqs. (10)–(12) are derived by integrating the angular dependence of the ingoing Stokes parameters in full analogy with what happens in the case when the magnetic field is absent [3] (see also [7] for further details as well as [8] for slightly different perspectives on magnetized photon-electron scattering). Note that

$$f_{\rm e}(\omega) = \frac{\omega_{\rm Be}}{\omega} = 2.79 \times 10^{-12} \biggl(\frac{B_{\rm u}}{\rm nG}\biggr) \biggl(\frac{\rm GHz}{\nu}\biggr) (z_{\rm rec} + 1), \qquad \omega_{\rm Be} = \frac{e|\vec{B} \cdot \hat{n}|}{m_{\rm e} a}, \tag{13}$$

where $\omega_{\rm B\,e}$ is the Larmor frequency and $B_{\rm u}$ denotes the uniform component of the comoving magnetic field intensity which is treated within the guiding centre approximation (see [9] for the description of magnetized plasma prior to recombination). The numerical solution of the system is greatly helped by exploiting systematically the integration along the line of sight [5] for all the brightness perturbations. From Eq. (4)

$$\Delta_{\rm V}(k, \mu, \omega, \tau_0) = \int_0^{\tau_0} \mathcal{K}(\tau)\, P_1(\mu) \biggl\{ f_{\rm e}(\omega) \biggl[2\Delta_{\rm I0} - S_{\rm P}\biggr] - \frac{3\,i}{4} \Delta_{\rm V1}\biggr\} e^{-i\mu k(\tau_0 - \tau)} d\tau, \tag{14}$$

[4] Note that $\omega_{\rm p\,e}/\omega_{\rm p\,i} = \sqrt{m_{\rm p}/m_{\rm e}}$ where $m_{\rm p}$ is the proton mass; $\omega = 2\pi\nu$ denotes throughout the angular frequency.

where $\mathcal{K}(\tau)$ is the visibility function and were $(\tau_0 - \tau)$ is effectively the (comoving) angular diameter distance in a spatially flat geometry. To zeroth order in the tight-coupling expansion Eq. (14) allows to evaluate the V-mode polarization, i.e.

$$\Delta_{\rm V}(k,\mu,\tau_0) = \frac{8}{3}\int_0^{\tau_0} \mathcal{K}(\tau) f_{\rm e}(\omega) e^{-i\mu k(\tau_0-\tau)}\, P_1(\mu)\, \overline{\Delta}_{\rm I0}(k,\tau)\, d\tau. \tag{15}$$

where $\overline{\Delta}_{\rm I0}(k,\tau)$ is the monopole of the intensity computed to lowest order in the tight coupling expansion, i.e. when the baryon velocity coincides with the dipole of the intensity of the radiation field. To lowest order in the tight coupling approximation the CMB is circularly polarized provided a large-scale magnetic field is present. The linear polarization is generated to first-order in the tight-coupling expansion but is larger than the V-mode polarization because of the smallness of $f_{\rm e}(\omega)$. More details on this semi-analytic discussion can be found in [7]. The evolution of the monopole of the intensity $\Delta_{\rm I0}$ can either be studied in the tight-coupling limit or it can be solved numerically. In both cases the initial conditions will be chosen to be adiabatic [5]

$$\Delta_{\rm I0}(k,\tau_{\rm rec}) = \frac{2(R_\nu+15)}{5(4R_\nu+15)}\mathcal{R}_*(k), \qquad \psi_*(k) = \biggl(1+\frac{2}{5}R_\nu\biggr)\phi_*(k), \tag{16}$$

where R_ν is the fractional contribution of the massless neutrinos to the radiation background and $\mathcal{R}_*(k)$ denotes the curvature perturbations prior to equality and for typical scales larger than the Hubble radius at the corresponding epoch. Since prior to equality $\mathcal{H} = 1/\tau$ we shall also have, from Eq. (5), that $\mathcal{R}_*(k) = -\psi_*(k) - \phi_*(k)/2$. For large angular scales (i.e. $\ell < 50$) the visibility function can be considered to be sharply peaked at recombination and it is in practice a Dirac delta function. The V-mode autocorrelation (i.e., for short, VV power spectrum) and the cross-corrrelation between polarization and temperature (i.e., for short, VT power spectrum) can then be computed analytically in this regime and the result [6] can be written as:

$$G_\ell^{\rm (VV)}(\omega) = \frac{256\pi}{225}\biggl(\frac{R_\nu+15}{4R_\nu+15}\biggr)^2 f_{\rm e}^2(\omega)\mathcal{A}_{\mathcal{R}}\biggl(\frac{k_0}{k_{\rm p}}\biggr)^{n_{\rm s}-1}\mathcal{I}_\ell^{\rm (VV)}(n_{\rm s}), \tag{17}$$

$$G_\ell^{\rm (VT)}(\omega) = \frac{16\pi}{75}\frac{(R_\nu+15)(2R_\nu-15)}{(4R_\nu+15)^2} f_{\rm e}(\omega)\mathcal{A}_{\mathcal{R}}\biggl(\frac{k_0}{k_{\rm p}}\biggr)^{n_{\rm s}-1}\mathcal{I}_\ell^{\rm (VT)}(n_{\rm s}), \tag{18}$$

[5] See, e.g., [6]. The present considerations can be straightforwardly generalized to the case of non-adiabatic initial conditions [10]. For a discussion on the peculiar features of the adiabatic and non-adiabatic initial conditions of the Einstein-Boltzmann hiererchy see, for instance, [11].

[6] For simplicity the angular power spectrum shall be denoted as $G_\ell^{\rm (XY)} = \ell(\ell+1)C_\ell^{\rm (XY)}/(2\pi)$. The VV and VT power spectra are the analog of the EE and TE power spectra arising in the case of the linear polarization. The temperature (related to the I Stokes parameter) and the circular polarization (related to the V- Stokes parameter) are both invariant under a rotation orthogonal to the direction of propagation of the radiation, as stressed after Eq. (1). It is therefore natural, in a first approach to the problem, to consider the TT, VT and the VV power spectra. Furthermore, the VT correlations are larger than the the VE and VB correlations.

where $k_0 = (\tau_0 - \tau_{\rm rec})^{-1}$ and $k_{\rm p} = 0.002$ Mpc^{-1} is the pivot scale while $\mathcal{A}_{\mathcal{R}}$ is the amplitude of the power spectrum of curvature perturbations at $k_{\rm p}$ (in the concordance paradigm and in the light of the WMAP data alone $\mathcal{A}_{\mathcal{R}} = (2.41 \pm 0.11) \times 10^{-9}$); the functions $\mathcal{I}_{\ell}^{({\rm VV})}(n_{\rm s})$ and $\mathcal{I}_{\ell}^{({\rm VT})}(n_{\rm s})$ appearing in Eqs. (17) and (18) are nothing but:

$$\mathcal{I}_{\ell}^{({\rm VV})}(n_{\rm s}) = \frac{\ell(\ell+1)[4\ell(\ell+1) - (n_{\rm s}-1)(n_{\rm s}-2)(n_{\rm s}-4)]\Gamma(3-n_{\rm s})\Gamma\left(\ell - \frac{3}{2} + \frac{n_{\rm s}}{2}\right)}{2^{6-n_{\rm s}}\Gamma\left(2-\frac{n_{\rm s}}{2}\right)\Gamma\left(3-\frac{n_{\rm s}}{2}\right)\Gamma\left(\frac{7}{2}+\ell-\frac{n_{\rm s}}{2}\right)}$$

$$\mathcal{I}_{\ell}^{({\rm VT})}(n_{\rm s}) = \frac{\ell(\ell+1)(2-n_{\rm s})\Gamma\left(2-\frac{n_{\rm s}}{2}\right)\Gamma\left(\ell+\frac{n_{\rm s}}{2}-1\right)}{4\sqrt{\pi}\Gamma\left(\frac{5}{2}-\frac{n_{\rm s}}{2}\right)\Gamma\left(\ell-\frac{n_{\rm s}}{2}+3\right)}, \tag{19}$$

and arise as analytically solvable integrals of products of spherical Bessel functions and of their derivatives. Before discussing the relevant numerical results over small angular scales it is appropriate to mention here that circular polarization is often invoked as the result of the Faraday conversion[7] of linearly polarized radiation [12]. For the latter mechanism to operate, relativistic electrons must be present in the system and this can happen only as a secondary effect when CMB photons pass through magnetized clusters (see [12], last reference); this is however not the idea pursued here since the pre-decoupling plasma is cold and electrons are deeply non-relativistic. The V-mode polarization, as we showed, is induced by the magnetized plasma itself thanks to the presence of (adiabatic) curvature perturbations in the system. Absent one of these two components the VT and VV power spectra would vanish. If the initial conditions would not be adiabatic the V-mode polarization would still be present but with different physical features which will depend upon the specific non-adiabatic solution [10, 11]. For smaller angular scales (i.e. $\ell > 100$) it is mandatory to integrate numerically the system across decoupling. Some of the results are summarized in Fig. 1. The thin lines in both plots denote the V-mode autocorrelations while the thick lines denote the cross-correlation of the circular polarization anisotropies with the temperature inhomogeneities. The signal is larger for low multipoles and its shape reminds a bit of the temperature autocorrelations induced by the tensor modes of the geometry which reach their largest value for small ℓ and decay exponentially for $\ell > 90$. Defining as $r_{\rm T}$ the tensor to scalar ratio at the pivot scale $k_{\rm p}$ [1, 11], for $r_{\rm T} = 1$ the TT correlations induced by the tensor modes would be $\mathcal{O}(10^3)\,(\mu{\rm K})^2$ while the VT correlations are $\mathcal{O}(10^{-5})\,(\mu{\rm K})^2$ for the choice of parameters of Fig. 1 (see, for instance, plot at the right, dot-dashed curve). For the same choice of parameters the VT power spectra are of the order of the B-mode autocorrelation

[7] Faraday conversion (typical of relativistic jets) should not be confused with Faraday rotation. In the presence of relativistic electrons linearly polarized radiation can be Faraday converted into circularly polarized radiation [12]. Faraday rotation is instead a rotation of the polarization plane of the (linearly polarized) radiation: in practice it can convert E-modes into B-modes but it does not lead to circularly polarized photons (see, e.g. third and last references of [9]). Faraday conversion and Faraday rotation have also different dependences upon the magnetic field intensity and upon the frequency.

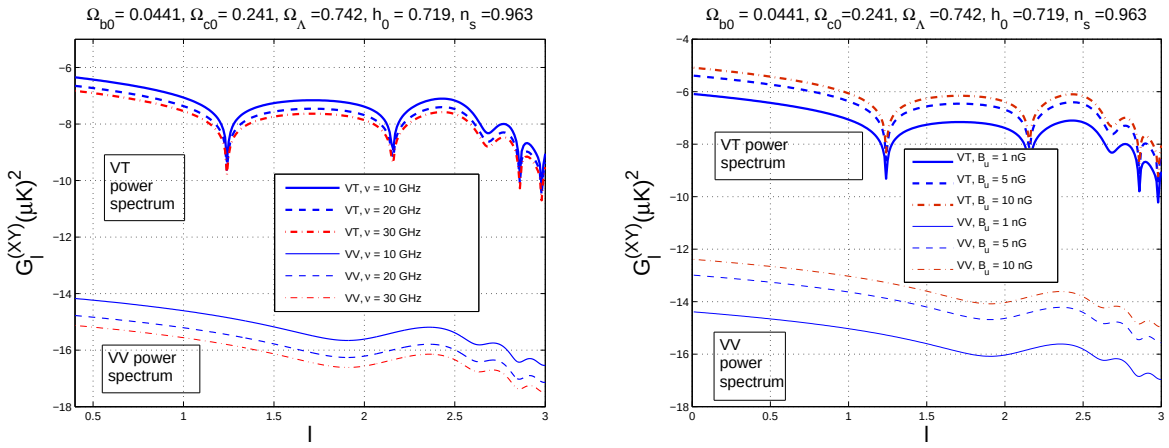

Figure 1: In the plot at the left the VT and the VV angular power spectra are reported for a fixed value of $B_{\rm u}$ (i.e. 1 nG) but for different values of the comoving frequency. In the plot at the right the comoving frequency is fixed to 10 GHz but the magnetic field strength increases. The thin lines denote the VV correlations while the thick lines denote the VT correlations. In the plots, on both axes, the common logarithm of the corresponding quantity is reported.

induced by the weak lensing of the primary anisotropies (i.e. $\mathcal{O}(10^{-5})(\mu{\rm K})^2$, see also left plot of Fig. 2 and the discussion below). By shifting the observational frequency the VT correlation can be even larger [13, 14]. The B-mode autocorrelation induced by the tensor modes of the geometry is typically larger, both than the V-mode polarization and than the BB spectra from lensing. For $r_{\rm T} \sim 0.1$, the BB angular power spectrum of the tensor modes of the geometry is $\mathcal{O}(10^{-2})(\mu{\rm K})^2$ for $\ell \sim 90$ corresponding to angular separations of roughly 2 deg. In Fig. 2 (plot at the left) the EE power spectrum stemming from the best fit to the WMAP 5-yr data alone is illustrated with a dashed line and compared, in the same plot, with the BB angular power spectrum arising from the lensing of the primary anisotropies (thin dot-dashed line) as well as with the V-mode autocorrelation (full thin curve at the bottom). The B-mode autocorrelation stemming from the tensor modes in the case $r_{\rm T} = 0.1$ is illustrated with the thick line. Always in Fig. 2 (plot at the right) the TE and the VT correlations are compared. Both in Figs. 1 and 2 the cosmological parameters are fixed (as indicated in the title of each figure) to the values of the best fit stemming from the WMAP 5-yr data alone in the light of the concordance model. In Fig. 2 the frequency of the channel has been taken of the order of 30 GHz. Even if the latter frequency is already rather low, it would be desirable to reduce it even more and to conceive spectropolarimetric measurements in the range of the GHz. The challenge of detecting the CMB radiation at low frequencies is neatly described in Ref. [13] where a set of absolute radiometers is employed in different channels at 0.6, 0.82 and 2.5 GHz (see also [14] for earlier results along the same theme). As specifically discussed also in analytic terms (see Eqs. (17)–(18)) the VV and VT power spectra are sensitive to

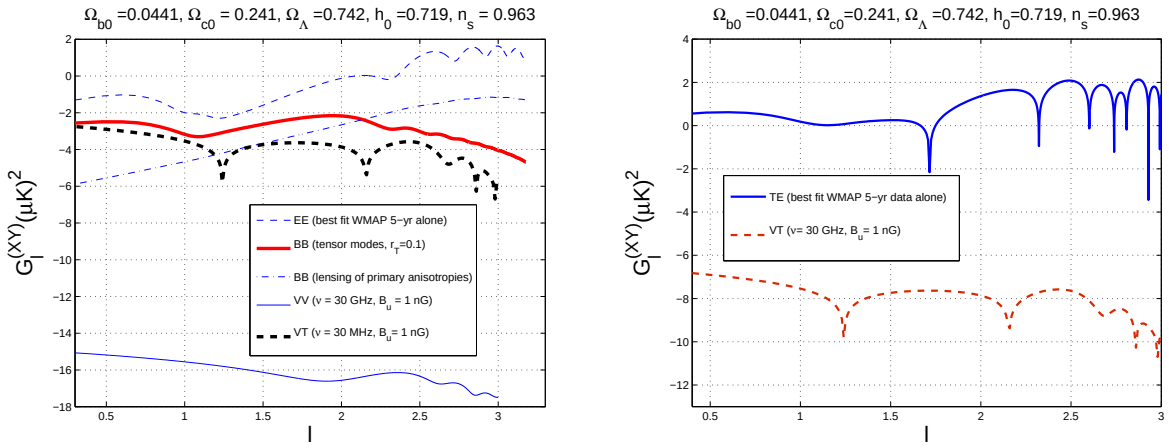

Figure 2: The V-mode power spectra are compared with the linear polarizations. As in Fig. 1 on both axes the common logarithm of the indicated quantity is reported.

the underlying cosmological parameters, to the initial conditions of the Einstein-Boltzmann hierarchy as well as to the magnetic field parameters. For illustration the concordance model supplemented by adiabatic initial conditions has been considered. The maximal intensity of the comoving magnetic field has been taken to be of the order of the nG. This is the range of current bounds stemming from the simultaneous analysis of the measured TE and TT power spectra (see [9], first and second reference). Larger magnetic fields would distort the acoustic oscillations in the TT power spectra. Low frequency instruments could make the difference for scrutinizing a potential V-mode polarization. In this respect the results and the techniques of [13] (as well as the earlier results of [14]) could be probably revisited in the light of the considerations developed here. It has been shown that the VT correlation for a comoving magnetic field from 5 to 10 nG can be as large as $10^{-5}\,(\mu\mathrm{K})^2$ at 10 GHz for $\ell < 20$ (i.e. large angular separations). This means that for frequencies $\mathcal{O}(\mathrm{MHz})$, the resulting signal could be even 6 or 7 orders of magnitude larger than a putative B-mode signal from gravitational lensing (see, e.g. Fig. 2, thick dashed curved in the left plot). It has been demonstrated that the study of circular dichroism is not more forlorn than other signals which are often invoked as conceptually important to consider but observationally difficult to assess. The systematic effects plaguing the measurements of the V-mode power spectra differ from the case of linear polarizations. Wether or not they are less severe depends also upon the features of the instrument and on the specific frequency band. The author is grateful to G. Sironi, M. Gervasi and A. Tartari for stimulating discussions.

References

[1] D. N. Spergel *et al.* [WMAP Collaboration], Astrophys. J. Suppl. **170**, 377 (2007); J. Dunkley *et al.* [WMAP Collaboration], Astrophys. J. Suppl. **180**, 306 (2009).

[2] H. Alfvén and C.-G. Fälthammer, *Cosmical Electrodynamics*, 2nd edn., (Clarendon press, Oxford, 1963).

[3] S. Chandrasekhar, *Radiative Transfer*, (Dover, New York, US, 1966).

[4] E. T. Newman and R. Penrose, J. Math. Phys. **7**, 863 (1966); J. N. Goldberg *et al.*, J. Math. Phys. **8**, 2155 (1967).

[5] M. Zaldarriaga and U. Seljak, Phys. Rev. D **55**, 1830 (1997); U. Seljak and M. Zaldarriaga, Astrophys. J. **469**, 437 (1996).

[6] E. Bertschinger, arXiv:astro-ph/9506070; C. P. Ma and E. Bertschinger, Astrophys. J. **455**, 7 (1995).

[7] M. Giovannini, arXiv:0909.4699 [astro-ph.CO].

[8] K. C. Chou, Ap. Space Sci. **121**, 333 (1986); B. Whitney, Astrophys. J. Suppl. **75**, 1293 (1991).

[9] M. Giovannini, Phys. Rev. D **79**, 121302 (2009); Phys. Rev. D **79**, 103007 (2009); M. Giovannini and K. Kunze, Phys. Rev. D **78**, 023010 (2008); M. Giovannini, Phys. Rev. D **74**, 063002 (2006); Phys. Rev. D **56**, 3198 (1997).

[10] R. Keskitalo, H. Kurki-Suonio, V. Muhonen and J. Valiviita, JCAP **0709**, 008 (2007); J. Valiviita and V. Muhonen, Phys. Rev. Lett. **91**, 131302 (2003).

[11] M. Giovannini, *A primer on the physics of the Cosmic Microwave Background*, (World Scientific, Singapore, 2008).

[12] A. G. Pacholczyk and T. L. Swihart, Astrophys. J. **150**, 647 (1967); V. N. Sazonov, Sov. Phys. JETP **29**, 578 (1969) [Zh. Eksp. Teor. Fiz. **56**, 1065 (1969)]; T. Jones and A. O'Dell, Astrophys. J. **214**, 522 (1977); A. Cooray, A. Melchiorri and J. Silk, Phys. Lett. B **554**, 1 (2003).

[13] M. Zannoni *et al.*, Astrophys. J. **688**, 12 (2008); M. Gervasi *et al.*, Astrophys. J. **688**, 24 (2008); A. Tartari *et al.*, Astrophys. J. **688**, 32 (2008).

[14] G. Sironi, M. Limon, G. Marcellino, G. Bonelli, M. Bersanelli, G. Conti, Astrophys. J. **357**, 301, (1990); G. Sironi, G. Bonelli, M. Limon Astrophys. J. **378**, 550 (1991).